Solvent- and Thermal-Induced Crystallization of Poly-L-Lactic Acid in Supercritical CO_2 Medium

Ana López-Periago, Carlos A. García-González, Concepción Domingo

Instituto de Ciencia de Materiales de Barcelona (CSIC), Campus de la UAB s/n, E-08193 Bellaterra, Spain

Received 6 November 2007; accepted 1 July 2008
DOI 10.1002/app.29111
Published online 3 October 2008 in Wiley InterScience (www.interscience.wiley.com).

ABSTRACT: The effect of different annealing treatments with supercritical carbon dioxide ($SCCO_2$) on the structural and mechanical properties of semicrystalline poly-L-lactic acid (L-PLA) was investigated. 2000, 27,000, 100,000, and 350,000 g mol^{-1} molecular weight L-PLA polymers were used in the study. The solid-state processing of L-PLA at temperatures lower than the effective melting point led to solvent- and thermal-induced crystallization. Solvent-induced and isothermal crystallization mechanisms could be considered similar regarding the increase of polymer chain mobility and mass-transfer in the amorphous region; however, quite different microstructures were obtained. $SCCO_2$ solvent-induced crystallization led to polymers with high crystallinity and melting point. On the contrary, $SCCO_2$ thermal-induced crystallization led to polymers with high crystallinity and low melting point. For these polymers, the hardness increased and the elasticity decreased. Finally, the effect of dissolving $SCCO_2$ in the molten polymer (cooling from the melt) was analyzed. Cooling from the melt led to polymers with high crystallinity, low melting point, low hardness, and low elasticity. Distinctive crystal growth and nucleation episodes were identified. This work also addressed the interaction of $SCCO_2$-drug (triflusal) solution with semicrystalline L-PLA.
 J Appl Polym Sci 111: 291–300, 2009

Key words: polylactic acid; supercritical; CO_2; crystallization; nucleation

INTRODUCTION

Polylactic acid (PLA) is an aliphatic polyester (—[O—CH(CH_3)CO]$_n$—) that has potential advantages for some specific applications, such as relative high mechanical strength, thermoplastic behavior, biodegradability, and biocompatibility.[1–4] Because of its high cost, PLA has been used mainly in the medical area and for specific purposes in the food industry to make plastic bags and bottles. The L-PLA isomer exists as a semicrystalline polymer, and its microstructural properties, mainly the molecular weight and degree of crystallinity, are of critical importance for its use in biomedical applications.[1] The construction of loaded bearing materials, such as screws and plates or scaffolds for use as orthopedic implants, needs tough materials with high hardness and, therefore, L-PLA with high molecular weight in the range of 10^5–10^6 g mol^{-1} and high crystallinity is desired.[5] On the other hand, the preparation of systems for their use in controlled drug release requires proper biodegradation characteristics, low crystallinity, and low molecular weight in the range of 10^3–10^4 g mol^{-1} to facilitate the incorporation of the drug to the polymer.[6]

In previous works,[7–12] various L-PLA microstructures and degrees of crystallinity have been described to be obtained by applying different processing conditions such as isothermal annealing, cooling from the melt, or solvent-induced crystallization. Particularly, solvent-induced crystallization led to L-PLA materials with a high degree of crystallinity. However, the described process is performed using organic solvents, which are difficult to eliminate from the final product. Hence, the resulting product could not be appropriate for their use in medical applications.

Technology based on supercritical carbon dioxide ($SCCO_2$) is considered as an alternative to overcome some of the problems associated with the use of traditional organic solvents for the preparation of pharmaceutical materials and biomaterials involving polymers.[13,14] $SCCO_2$ can be used either as media for polymer synthesis[15,16] or for the postmodification of polymer morphology.[17,18] The $SCCO_2$ induces depression in the glass transition (T_g), crystallization (T_c), and melting (T_m) temperatures of semicrystalline polymers, which has been reported to affect the crystallization kinetics.[19–24] Takada et al.[23] observed

Correspondence to: C. Domingo (conchi@icmab.es).
Contract grant sponsor: EU Project STRP SurfaceT; contract grant number: NMP2-CT-2005-013524.
Contract grant sponsor: Spanish MEC; contract grant numbers: MAT2005-25567-E, MAT2006-28189-E.
Contract grant sponsor: CSIC.

TABLE I
Characteristics of Polymers Employed

Sample	Supplier	Molecular weight, M_w (g mol^{-1})	Morphology
PLA_2	Lab synthesized	2,000	Powder
PLA_{27}	Lab synthesized	27,000	Powder
PLA_{100}	Biovalley	100,000	Pellets
PLA_{350}	Purac Biochem	350,000	Pellets

a $SCCO_2$-induced increase of the crystallization rate of L-PLA at the self-diffusion crystal-growth-controlled region (at $T < 122$°C) and a decrease at the nucleation-controlled region (at $T > 132$°C). This article is devoted to obtain general conclusions of the effect of L-PLA annealing under $SCCO_2$ and L-PLA crystallization behavior. This study was performed on various L-PLA polymers, ranging from low (2 kg mol^{-1}) to high (350 kg mol^{-1}) molecular weight processed at different crystallization conditions. We first analyzed the solid-state processing at temperatures lower than the L-PLA melting point; and, second, we studied the effect of dissolving $SCCO_2$ in the molten polymer.

Finally, this work also addressed the interaction of $SCCO_2$-drug (triflusal) solutions with low-molecular weight L-PLA. The objective was to prepare a drug delivery system based on the impregnation of the drug in the L-PLA matrix using $SCCO_2$ as a solvent.[13]

EXPERIMENTAL

Materials

Characteristics of the used polymers are shown in Table I. Low and medium molecular weight polymers (PLA_2 and PLA_{27}, respectively) were synthesized in our laboratories by step-growth polymerization of lactic acid,[2] whereas commercial high-molecular weight polymers (PLA_{100} and PLA_{350}) were commercially obtained. The drug used for attempting the molecular impregnation of L-PLA was 2-acetoxy-4-(trifluoromethyl)benzoic acid (triflusal). Triflusal and PLA_{350} were kindly donated by Uriach S.A. (Barcelona, Spain) and Purac Biochem (Gorinchem, The Netherlands), respectively.

Process and equipment

Experiments were performed in a high-pressure equipment running in the batch mode (Fig. 1). Cooled (Ex1) $SCCO_2$ was pressurized with a syringe pump (1, TharDesign SP240) and added to the reactor (2, TharDesign, 70 mL) until the working pressure (P) was reached. The reactor was heated at the chosen temperature (T) using resistances (Re1). The system was stirred (S1) at 300 rpm and the working conditions were maintained for 24 h. In a typical experiment, the reactor was charged with 1 g of polymer. At the end of each experiment, the system was depressurized at 0.2–0.4 MPa min^{-1} and led to cool to room temperature in air. The depressurization was controlled by means of a metering valve (V5) situated at the exit of the reactor. Samples were labeled $PLA_{M_w}SC$ ($P - T$), where M_w refers to the molecular weight of the polymer.

To contrast the effect of $SCCO_2$ on L-PLA polymer crystallization, samples of raw L-PLA were introduced in an air oven and heated at similar temperatures than those used for the supercritical batch experiments. Samples were labeled $PLA_{M_w}C(T)$.

A similar high-pressure setup was used to process L-PLA and triflusal together. In this case, the reactor was charged with 0.5 g of PLA_2 polymer and 0.5 g of triflusal. The mixture was pressurized with CO_2 at 10 MPa and 50°C for 24 h.

Characterization

The thermal properties of both the raw and treated L-PLA were analyzed using differential scanning calorimetry analysis (DSC, Mettler Toledo 822e/400). Samples weighting between 4 and 6 mg were heated at a rate of 10°C min^{-1} from 20 to 250°C under 50 mL min^{-1} N_2 purge. Several PLA_2 samples were also measured at a heating rate of 2°C min^{-1}. The information from the DSC curves was

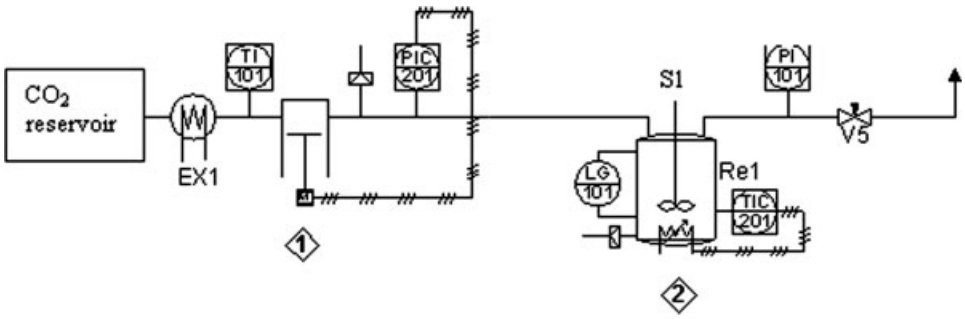

Figure 1 Schematic equipment setup.

TABLE II
Experimental Working Conditions and ^{1}H NMR and DSC Analysis Results

Sample	Annealing	P (MPa)	T (°C)	^{1}H NMR (ppm)	T_g (°C)	T_c (°C)	T_m (°C)	ΔH_m (J g^{-1})	X_c
PLA_{350}raw	–	–	–	5.20; 1.52	53	No	189	75	80
PLA_{350}SC(10–50)	CO_2	10	50	5.20; 1.52	68	No	194	79	84
PLA_{350}SC(20–50)	CO_2	20	50	5.20; 1.52	68	No	192	78	82
PLA_{350}SC(12–120)	CO_2	12	120	5.20; 1.52	No	No	186	88	95
PLA_{350}C(50)	Air	0.1	50	5.20; 1.52	54	No	189	73	78
PLA_{350}C(120)	Air	0.1	120	5.20; 1.52	No	No	191	77	80
PLA_{100}raw	–	–	–	5.20; 1.52	47	No	176	47	50
PLA_{100}SC(12–120)	CO_2	12	120	5.20; 1.52	No	No	173	71	76
PLA_{27}raw	–	–	–	5.20; 1.52 4.39; 1.51	44	Yes	184	–	–
PLA_{27}SC(10–50)	CO_2	10	50	5.20; 1.52 4.39; 1.51; 4.00	46	Yes	193	–	–
PLA_{27}SC(20–50)	CO_2	20	50	5.20; 1.52 4.39; 1.51; 4.00	46	Yes	198	–	–
PLA_{27}C(50)	Air	0.1	50	5.20; 1.52 4.39; 1.51	42	Yes	188	–	–
PLA_{27}C(120)	Air	0.1	120	5.20; 1.52 1.51	64	No	148	–	–
PLA_2raw	–	–	–	5.20; 1.52	35	Yes	143	–	–
PLA_2SC(20–50)	CO_2	20	50	5.20; 1.52	No	No	145	70	75
PLA_2C(50)	Air	0.1	50	5.20; 1.52 1.51	38	Yes	145	–	–
PLA_2C(120)	Air	0.1	120	5.20; 1.52 1.51	No	No	151	76	82

used to determine the onset of T_g, as well as T_c and T_m transition peaks. The thermal stability of several samples was evaluated using thermogravimetric analysis (TGA, Perkin-Elmer 7) under N_2 atmosphere in the range 20–900°C and raising the temperature at a rate of 5°C min^{-1}. Purity and composition of raw and processed samples were determined by ^{1}H nuclear magnetic resonance (^{1}H NMR, Bruker ARX-300 MHz). A Nano Indenter XP testing machine from MTS Nano Instruments was used to acquire samples mechanical data (hardness and Young's modulus) on the submicron scale. Testing based on pyramidal Berkovich tips was conducted at room temperature. Each measured data was an average of 10 indents. Materials were loaded to a maximum load of $\sim$ 100 mN. The morphological analysis was performed with a Hitachi S570 scanning electron microscope (SEM). The sample crystallinity was examined using X-ray diffraction (XRD) with a Rigaku Rotaflex RU200 B instrument.

RESULTS AND DISCUSSION

Studied L-PLA samples were prepared by annealing different polymers of high (350 and 100 kg mol^{-1}), medium (27 kg mol^{-1}), and low (2 kg mol^{-1}) molecular weight at several temperatures during 24 h under either $SCCO_2$ or air atmosphere (Table II). The used temperatures were specifically chosen to be close to either the glass transition temperature of L-PLA (50°C) or the polymer melting temperature (120°C). In the first case, a solvent or thermal-induced competitive crystallization effect was expected, whereas in the second, crystallization from the melt was more likely to occur.

Polymers stability under working conditions

First, the effect that the used pressure and temperature during experiments produced on the stability of the different L-PLA polymers was studied. The composition and degradation characteristics of the processed L-PLA samples were examined using ^{1}H NMR spectroscopy. Results are presented in Table II and Figure 2. The ^{1}H NMR spectrum of pure L-PLA is constituted by two set of signals at 5.20 and 1.52 ppm corresponding to the methine proton (quartet) and the protons of the methyl group (doublet), respectively.[25] Raw PLA_{350} [Fig. 2(a)], PLA_{100} [Fig. 2(b)], and PLA_2 [Fig. 2(d)] only displayed these set of signals, indicating that they were pure compounds. However, the ^{1}H NMR spectrum of the raw PLA_{27} [Fig. 2(c)] showed the two mentioned set of signals and another set of less intense signals (at 4.39 and 1.51 ppm) corresponding to L-PLA oligomers of unidentified molecular weight, likely coming from polymer degradation.[26] Despite the presence of these two extra set of signals, the abundance of non-degraded polymer in the raw PLA_{27} was estimated to be $\sim$ 90 wt %. The reason behind this degradation could lay in the method employed for PLA_{27} synthesis, as well as in the time and storing conditions.[27–29]

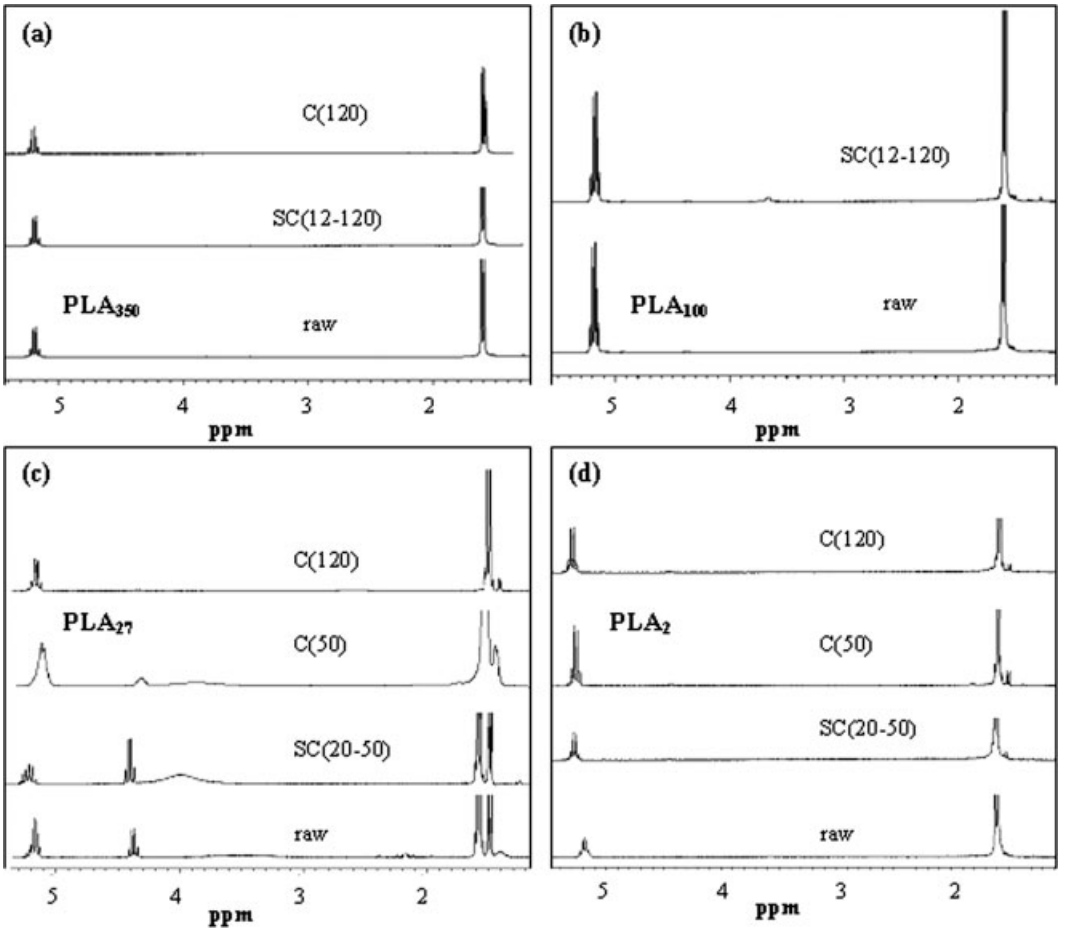

Figure 2 ^{1}H NMR spectra of raw and processed L-PLA polymers treated at either 50 or 120°C under supercritical conditions and under atmospheric air: (a) PLA_{350}; (b) PLA_{100}; (c) PLA_{27}; and (d) PLA_2.

The obtained ^{1}H NMR spectra of the processed, either supercritical or conventional, high-molecular weigh PLA_{350} and PLA_{100} pellets [Fig. 2(a,b), respectively] did not show any changes in the chemical shifts or in the multiplicity of the signals with respect to the raw materials, even when annealed at the high temperature of 120°C, indicating that the performed treatments did not induce degradation in these polymers. The ^{1}H NMR spectrum of the processed PLA_2 under supercritical conditions at 20 MPa and 50°C [sample PLA_2SC(20–50) in Fig. 2(d)] was similar to the one of the raw PLA_2. Incipient thermal degradation was observed only when annealing PLA_2 in air at either 50 or 120°C [Fig. 2(d)]. On the other hand, the ^{1}H NMR spectra of the processed PLA_{27} samples showed changes in the multiplicity and integration of the displayed signals in comparison with the ones observed in the raw material [Fig. 2(c)]. The spectrum of the $SCCO_2$ processed PLA_{27} sample at 20 MPa and 50°C [sample PLA_{27}SC(20–50)] showed two sets of multiplets at 5.20 and 4.40 ppm. In the same way, the two observed doublets at 1.52 and 1.51 ppm in the raw material developed into two multiplets in the processed sample. Moreover, a broad band at 4.00 ppm was observed in the spectrum, which could correspond to the OH group of the lactic acid. For the sample PLA_{27}SC(20–50), a percentage of $\sim$ 40 wt % of nondegraded PLA_{27} was estimated. A similar feature was observed on sample PLA_{27}SC(10–50) [not shown in Fig. 2(c)], where the integration of the two set of multiplets revealed a percentage of $\sim$ 50 wt % of nondegraded PLA_{27}. ^{1}H NMR spectrum of the air-annealed sample at 50°C showed that the percentage of the low-molecular weight polymers (20 wt %) remained similar to that in the raw material (10 wt %). Therefore, the PLA_{27} degradation was much faster under supercritical working conditions by performing a similar annealing at 50°C in an air oven [sample PLA_{27}C(50) in Fig. 2(c)]. It should be taken into account that the pH is an important factor in the hydrolytic degradation of L-PLA, which is catalyzed by both acid and basic conditions.[1] Hence, degradation was enhanced when treating the sample under $SCCO_2$ conditions, since the CO_2 interaction with the PLA_{27} residual water caused the acid-catalyzed hydrolysis. Indeed, at 50°C, the degradation process was observed to be more significant at 20 MPa than at 10 MPa,

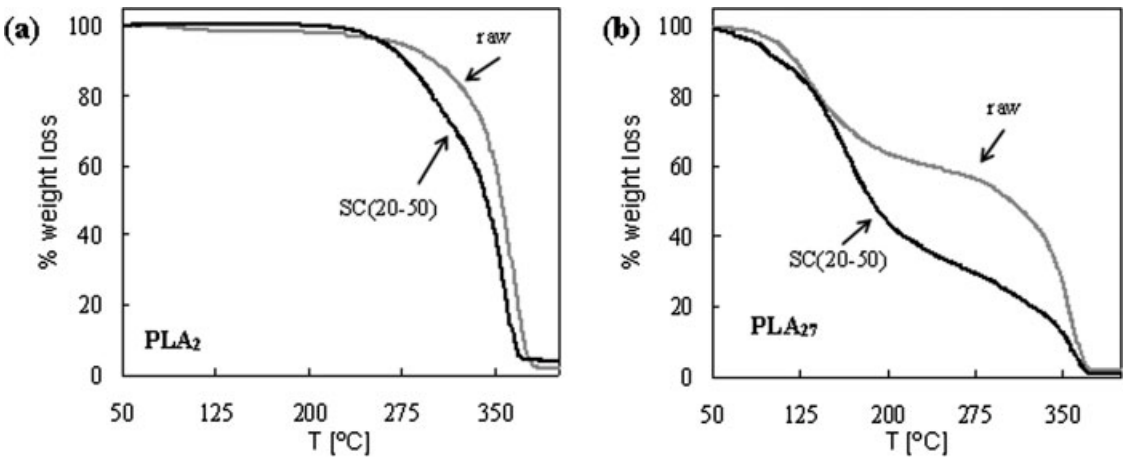

Figure 3 TGA analysis of medium and low-molecular weight L-PLA polymers either raw or treated at 50°C under 20 MPa of $SCCO_2$: (a) PLA_2 and (b) PLA_{27}.

supporting the idea of an accelerated degradation process due to CO_2 presence.

To further study the observed degradation behavior of PLA_{27} polymer samples, a thermogravimetric analysis was performed and its behavior was compared with that of PLA_2. Residual weight as a function of temperature is shown in Figure 3(a,b) for PLA_2 and PLA_{27}, respectively. For raw PLA_2 samples, TGA curve corresponded to the typical one-stage decomposition of a 100% L-PLA polymer in volatile products with the overall loss of weight between 250 and 375°C [Fig. 3(a)].[30] However, PLA_{27} decomposed with two well-resolved decays [Fig. 3(b)], indicating that there were at least two phases in the raw polymer with a different thermal stability. The first decay (weight loss 40 wt %) started at 100°C (which could correspond to water in the sample) and it was very much significant at $\sim$ 122°C (near the boiling point of lactic acid and small oligomers). The second decay (250–325°C) was similar to that observed for PLA_2 thermal decomposition. For sample PLA_{27}SC(20–50), the percentage of the less thermally stable phase increased considerably supporting the hypothesis of ^{1}H NMR analysis of acid-catalyzed degradation during $SCCO_2$ treatment.

For the crystallization study, the treatment at 120°C was only applied to the high-molecular weight L-PLA polymers, since the medium- and low-molecular weight polymers were highly degraded under these conditions.

Solvent-induced crystallization (crystal growth)

It is generally acknowledged that, in the presence of certain interactive liquids or gases, crystallization of semicrystalline polymers can take place at temperatures well below their crystallization transition temperature (T_c) through a solvent-induced crystallization process.[31,32] The course of the solvent-induced crystallization process starts with the sorption and diffusion of the fluid into the amorphous part of the polymer leading to plasticization and an increase of free volume. Then, the process continues by the rearrangement of the molecules toward a crystalline condition. A similar effect was expected in a polymer $SCCO_2$–solvent-induced crystallization process, since CO_2 at high pressure resembles common organic solvents in its ability to swell and plasticize polymers.[21–24] The effect was studied in this work by annealing the high PLA_{350} and medium PLA_{27} molecular weight polymers at 50°C (temperature well below the usual crystallization temperature of L-PLA: 100–110°C) under either 10 or 20 MPa of CO_2.

Melting transitions for raw and treated high-molecular weight PLA_{350} are shown in Figure 4(a). The DSC thermograph carried out up to 250°C of the raw PLA_{350} pellets showed two distinct endothermic thermal transitions (Table II). First, a small band was observed that corresponded to the glass transition at 53°C [not shown in Fig. 4(a)]. This was followed by a second sharp peak at 189°C corresponding to the melting point [Fig. 4(a)]. For this polymer, the area below the melting peak was used to calculate the enthalpy of melting (ΔH_m) and the degree of crystallinity (X_c) relative to the enthalpy of melting for a enantiopure L-PLA of 100% crystallinity (ΔH_m^0): $X_c = \Delta H_m/\Delta H_m^0$. A value of 93 J g^{-1} was used for ΔH_m^0.[33] For raw PLA_{350}, the crystallinity was estimated to be 80%. Both, the melting enthalpy and the melting point, of PLA_{350}, increased after supercritical treatment at 50°C under $SCCO_2$ at either 10 [sample PLA_{350}SC(10–50)] or 20 MPa [samplePLA_{350}SC(20–50)] (Table II). The raise of the melting point can be understood as an augment in crystallite size and/or in the polymer crystalline perfection. The increment on T_g values of $\sim$ 15°C (Table II), which accompanied the increment of T_m, was attributed to an increase in the crystallinity after treatment. For both

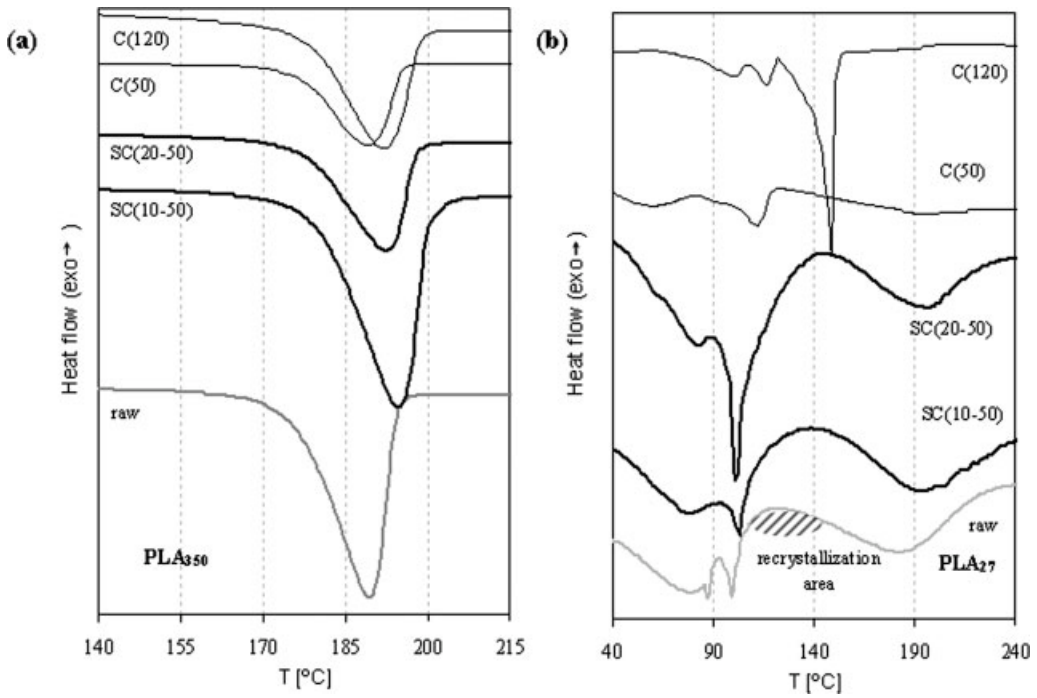

Figure 4 DSC analysis (heating rate 10°C min^{-1}) of high and medium molecular weight L-PLA polymers: (a) PLA_{350} and (b) PLA_{27}.

recovered samples, the crystallinity increased to about 4%. A similar behavior to that of PLA_{350} in regard of a rise in the melting temperature was observed for PLA_{27} when treated at 50°C under $SCCO_2$ at either 10 or 20 MPa (Table II). However, raw PLA_{27} polymer had a large amorphous fraction and exhibited, in addition to the endothermic T_g and T_m transitions, an exothermic cold crystallization transition [Fig. 4(b)]. For this polymer, no attempt was made to determine the degree of crystallinity from DSC-registered curves, since band broadening led to the overlap of exothermic and endothermic transitions. Additionally, DSC analysis also showed the partial degradation of raw PLA_{27} polymer by the development of several melting peaks at low temperatures ($\sim$ 100°C) before the cold crystallization/melting area. These low-temperature endothermic peaks may be the result of melting of crystallites constituted by randomly hydrolyzed degradation fragments (oligomers) trapped in the amorphous matrix.[34] When raw PLA_{27} was treated under $SCCO_2$ conditions at 50°C, the percentage of low-molecular weight phases [estimated using the area below the low-molecular weight melting peaks of samples PLA_{27}(10–50) and PLA_{27}(20–50) in Fig. 4(a)] increased, corroborating previously obtained ^{1}H NMR data.

For PLA_{350} and PLA_{27}, the annealing effect on the melting temperature and crystallinity at 50°C was merely noneffective by performing the process in the absence of $SCCO_2$ (Table II). Experiments carried out with PLA_{350} in air indicated that to reach a similar effect than that obtained under $SCCO_2$ conditions regarding the increase of polymer crystallinity and melting point, the temperature must be raised to 120°C [sample PLA_{350}C(120) in Fig. 4(a)]. When PLA_{27} was heated at 120°C in the absence of $SCCO_2$ [sample PLA_{27}C(120) in Fig. 4(b)], the DSC thermograph only showed the low-molecular weight melting points indicating that the sample was completely degraded.

Nanoindentation measurements were used to characterize the near-surface mechanical properties[35] of the PLA_{350} polymer [Fig. 5(a)]. The obtained elasticity modulus and hardness values for raw PLA_{350} were of 1.1 and 5.2 GPa, respectively. The hardness and elongation increase (Young's modulus decrease) observed after supercritical treatment at either 10 or 20 MPa of $SCCO_2$ and 50°C was due to the increasing crystallinity. This is a typical behavior of ductile materials, i.e., when crystallinity increases the hardness raises, but the ductile material is more easily deformed because of the generation of more dislocations.[36,37]

The solvent-induced crystallization process is controlled by the diffusion of the solvent into the polymer and, hence, $SCCO_2$ provides advantages since the amount of adsorbed gas and the diffusion coefficient can be continuously increased by elevating the pressure. However, in our experiments no significant differences were observed in the increase of crystallinity and melting point of the PLA_{350} and PLA_{27} polymers by increasing the CO_2 pressure from 10 to 20 MPa (Table II) when maintaining the temperature

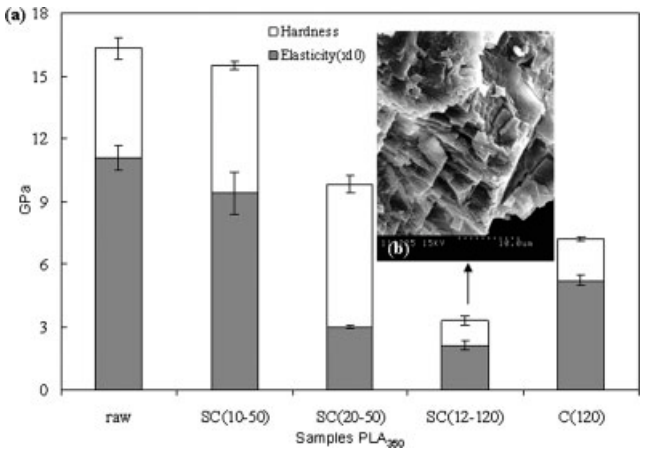

Figure 5 Mechanical and morphological properties of PLA_{350} samples: (a) Young's module and hardness (the origin of the hardness on the graph is located at the apex of the column of Young's module); and (b) SEM micrograph of a fractured piece of the sample $PLA_{350}SC(12–120)$.

at 50°C. On the other hand, in terms of mechanical properties, the annealing effect for the PLA_{350} polymer was more significant in the sample treated at 20 MPa than in the sample treated at 10 MPa [Fig. 5(a)].

Thermal-induced crystallization and cooling from the melt (nucleation)

At temperatures higher than the polymer's glass transition, isothermal crystallization may precede the solvent-induced crystallization process. The rapid heat transfer in thermal-induced crystallization relative to diffusion mass transport in solvent-induced crystallization provoked that the L-PLA reacted to the input of sensible heat before any significant solvent penetration had taken place.[38,39] Thermal-induced crystallization was first studied in this work by treating the high-molecular weight polymers PLA_{350} and PLA_{100} at 120°C under 12 MPa of $SCCO_2$. For the low-molecular weight PLA_2 polymer, annealing effects were analyzed at 50°C.

Figure 6(a) shows a collection of raw and treated PLA_{350} and PLA_{100} DSC thermographs. Treatment under $SCCO_2$ at 12 MPa and 120°C [sample $PLA_{350}SC(12–120)$ in Fig. 6(a)] enabled the raw PLA_{350} to crystallize fully as evidenced by an increase in crystallinity to 95% from the original value of 80% for the raw material (Table II). However, the $SCCO_2$ treatment of PLA_{350} at 120°C depressed the melting point significantly. Similar results were obtained for PLA_{100} [sample $PLA_{100}SC(12–120)$ in Fig. 6(a)]. The PLA_{100} crystallinity increased from 50% in the raw material to 76% in the treated one, whereas the melting point decreased from the original value of 176 to 173°C (Table II). For both high-molecular weight polymers, the decrease in the melting point value indicated the formation of smaller crystals and a less organized crystalline structure in comparison with the raw materials, even though an increase on the crystallinity was also observed. Since both polymers were

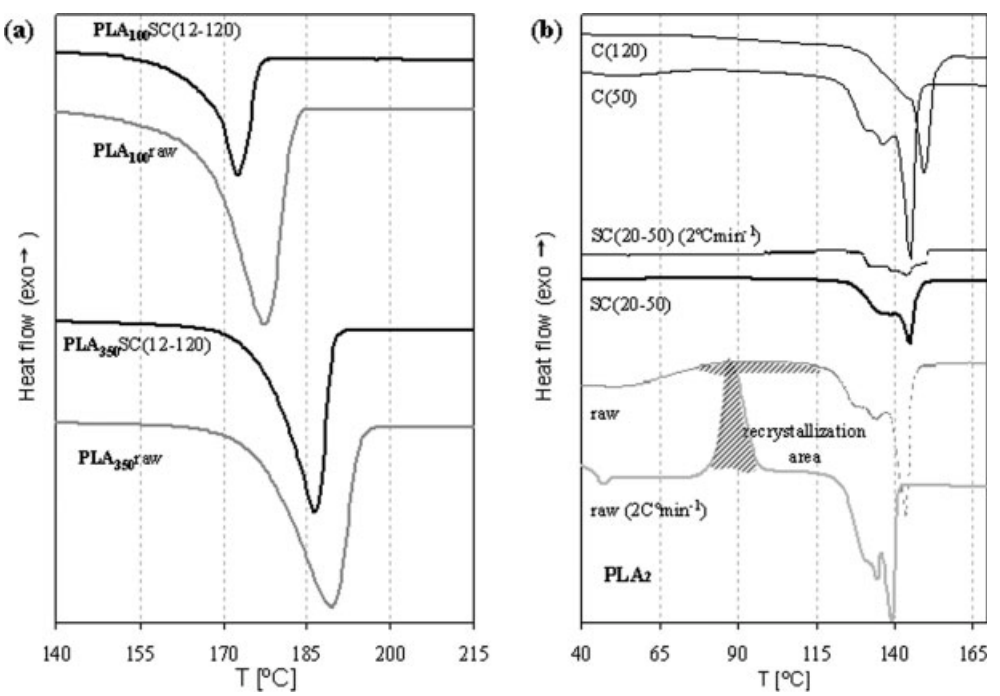

Figure 6 DSC analysis (heating rate 10°C min^{-1}) of high and low-molecular weight L-PLA polymers: (a) PLA_{350} and PLA_{100}; and (b) PLA_2 [samples of raw PLA_2 and $PLA_2SC(20–50)$ also registered at 2°C min^{-1} heating rate].

initially highly crystalline, the formation of a less organized crystalline structure has to be carried out through a recrystallization process, i.e., they first melted and then nucleated again. The melting happened because the interaction of the polymers with $SCCO_2$ lowered the effective melting temperature from the original values of 189 and 176°C for PLA_{350} and PLA_{100}, respectively, at least up to 120°C. Upon $SCCO_2$ expansion at the end of the experiments, the melted samples experienced sudden pressure and temperature drops and the chain molecules reassociate fast, leading to a rapid formation of nuclei and, therefore, a small size of spherulites and low organized crystalline regions. Raw high-molecular weight L-PLA pellets (PLA_{350} and PLA_{100}) were stress-induced (oriented) crystallized materials and, thus, transparent. After processing, samples PLA_{350}SC(12–120) and PLA_{100}SC(12–120) developed white color. The observed change in appearance for PLA_{350} and PLA_{100} also underlined a transition to a quiescent nucleated material.[1]

In regard of the mechanical properties, PLA_{350} treated at 12 MPa and 120°C showed lower hardness and higher elongation than the raw material [Fig. 5(a)]. This appears to indicate that the sample failure mode changed from the ductile fracture in raw PLA_{350} to brittle fracture in treated PLA_{350}SC(12–120). For this sample, a brittle transgranular fracture was observed in the SEM photographs [Fig. 5(b)], where the formation of the lamellar stacks with stepped topography was attributed to the occurrence of melting during the $SCCO_2$ treatment and recrystallization during expansion. The mechanical properties in this work were measured using a nanoindenter. It should be pointed out that obtained results using this technique can be different to that obtained for macromechanical properties measured using conventional indenters. This is due to the effects that may be introduced by geometrical nonlinearity on the surface at the nanoscale. In our case, for the crystallized polymer with brittle fracture, the characterization of the surface down to the level of a few nanometers also involves the description of the interphase between the lamellar stacks and not only (or with preference to) the bulk of the constituent crystals. Interphase is generally found to be significantly softer than the bulk. Therefore, direct comparison between values obtained for raw PLA_{350} with ductile fracture and sample PLA_{350}SC(12–120) with brittle fracture cannot be performed.[40]

The low-molecular weight raw PLA_2 had a significantly lower melting point (145°C) than the high-molecular weight L-PLA polymers (~ 180°C) (Table II). DSC thermographs showed that for the raw PLA_2, the endothermic glass transition (~ 35°C) was followed by an exothermic cold crystallization peak [Fig. 6(b)]. The cold crystallization exotherm (registered at 2°C min^{-1} heating rate) had a heat content that corresponded to ~ 70% of the heat content of the melting endotherm and, therefore, it was estimated that the raw PLA_2 was constituted by ~ 30% of crystallized polymer. No significant effect in regard of the melting point was observed after heating the sample at 50°C either under 20 MPa of $SCCO_2$ [sample PLA_2SC(20–50)] or in air [sample PLA_2C(50)]. However, the endothermic glass transition and the exothermic cold crystallization peak were not observed in the DSC-registered curve of the $SCCO_2$ treated sample, even when performing the DSC analysis at 2°C min^{-1}, indicating crystallization of the amorphous part. The new crystallinity value for the supercritical treated sample was calculated to be 75% (Table II). Hence, for the PLA_2 a thermal annealing took place even at the low temperature of 50°C, since the interaction of $SCCO_2$ with the polymer lowered the effective T_g and T_m and, thus, also the T_c, placing the PLA_2 in the crystallization temperature domain. Crystallites already immersed in the amorphous part of the raw semicrystalline PLA_2 may act as nuclei during the $SCCO_2$ thermal annealing process, which lowered the nucleation energy. Under air, T_g and T_c only vanished after heating the sample at 120°C [sample PLA_2C(120) in Fig. 6(b)].

Effect of $SCCO_2$ on L-PLA crystallization at different temperatures

The treatment with $SCCO_2$ at different temperatures allowed obtaining L-PLA samples having different structures with respect to the crystallinity, crystallite size, and crystal morphology. Three different behaviors, schematized in Figure 7, were observed as a function of processing temperature.

Solvent-induced crystallization

When the sample was crystallized at temperatures close to the glass transition temperature of the raw polymer -T_g(raw)-. The used temperature (T_1 in Fig. 7) was higher than the effective glass transition temperature of the polymer under the applied pressure of CO_2 -T_g($SCCO_2$)-, but lower than the T_g(raw). Both the melting point and the polymer crystallinity increased after processing. In this case, the mass transport at the interface between the amorphous and crystalline phases was facilitated due to the plasticizing effect of $SCCO_2$. The system was in the crystal-growth rate-controlled region, where the magnitude of the effect of $SCCO_2$ on the self-diffusion of polymer chain at the interface was dominant over the nucleation rate in the amorphous region.

Isothermal-induced annealing

When the sample was crystallized at temperatures between the glass transition temperature -T_g(raw)-

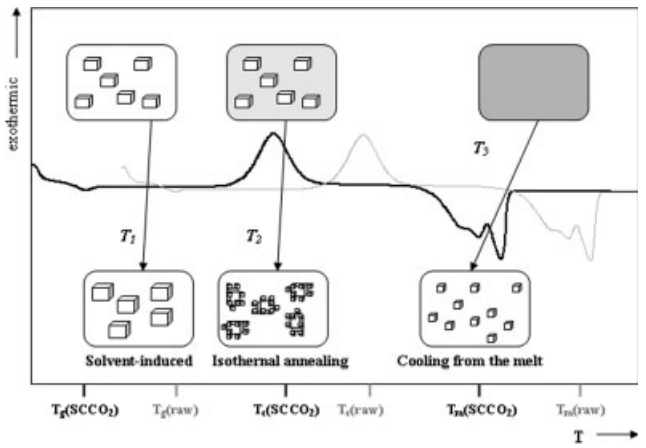

Figure 7 Schematic description of the possible L-PLA annealing processes as a function of temperature.

and cold crystallization temperature -T_c(raw)- of the raw polymer, the used temperature (T_2 in Fig. 7) was in the range of the effective cold crystallization temperature of the polymer under the applied pressure of CO_2 -T_c($SCCO_2$)-, but lower than the T_c(raw). The crystallinity of the sample increased but the melting point decreased indicating the formation of small crystals, likely coming from a nucleation episode. In this case, the nonspecific chain–chain interactions in the amorphous domain were reduced by the presence of $SCCO_2$ and the polymer chains rearranged themselves into the crystalline lower free energy state. The system was in the nucleation rate-controlled region. The presence of L-PLA crystallites dispersed in the $SCCO_2$-plasticized amorphous domain reduced the nucleation energy, leading to a seeded nucleation.

Cooling from the melt

When the sample was crystallized at temperatures between the cold crystallization temperature -T_c (raw)- and the melting point -T_m(raw)- of the raw polymer, the used temperature (T_3 in Fig. 7) was superior to the effective melting temperature of the polymer under the applied pressure of CO_2 -T_m ($SCCO_2$)-, but lower than the T_m(raw). The crystallinity of the obtained sample increased but the melting point decreased indicating small crystals and a nucleation episode. In this case, polymer crystallization took place after an episode of nucleation from the melt induced during system depressurization and cooling.

PLA_2 and triflusal system

For the preparation of polymeric drug-dispersed delivery systems, polymers impregnation using supercritical fluid technology has proven to be feasible when the pharmaceutical compound is soluble in $SCCO_2$ and the polymer can be swollen by the supercritical fluid.[41] The impregnation process is, thus, based on the polymer plasticization by $SCCO_2$, followed by active agent infusion into the polymeric phase. In this work, PLA_2 polymer was chosen to carry out the impregnation experiments, since it has a large amorphous part, which can be swollen by $SCCO_2$. The used active agent, the triflusal, has a chemical structure similar to that of aspirin, but with an additional trifluoromethyl group, that renders the resultant fluorinated compound very soluble in $SCCO_2$. PLA_2 was treated under a $SCCO_2$-triflusal solution at 10 MPa and 50°C. The ^{1}H NMR spectrum of the recovered sample showed the distinctive triflusal and L-PLA signals [Fig. 8(a)]. The estimated amount of triflusal on PLA_2 was 13 wt %. The XRD spectra showed the diffraction lines of the α-form of L-PLA and the main triflusal signal at $2\theta = 19.8°$, proving that both compounds were present in the sample in the crystalline form [Fig. 8(b)]. The SEM micrographs of the sample showed that the surface of the PLA_2 polymer was covered of triflusal crystals [Fig. 8(c)]. Hence, the obtained formulation was a recrystallized drug deposited on the polymer matrix and not an impregnated system. For semicrystalline

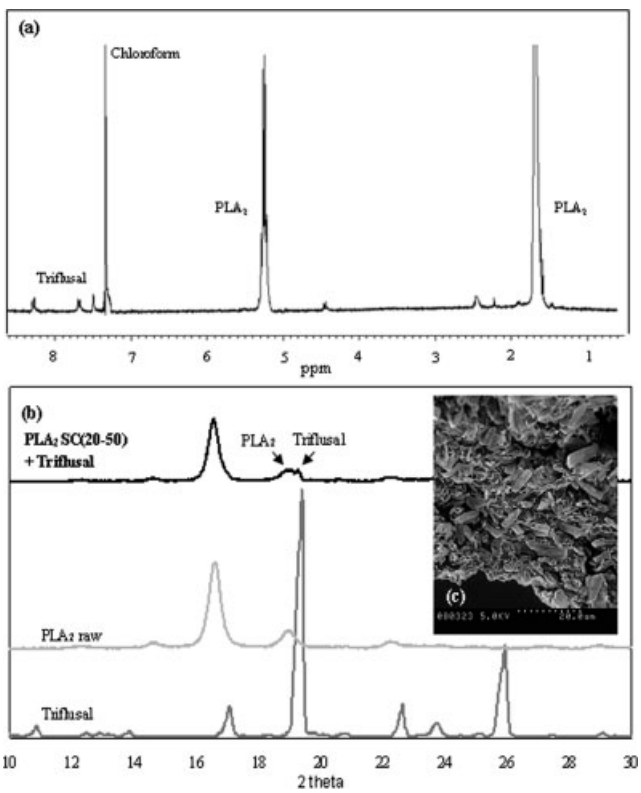

Figure 8 Analysis of the supercritically obtained sample of PLA_2 and triflusal in $SCCO_2$ at 10 MPa and 50°C: (a) ^{1}H NMR spectrum of the processed mixture; (b) XRD diffraction patterns of PLA_2, triflusal, and the processed mixture; and (c) SEM micrograph of the processed mixture.

polymers such as L-PLA, the induced nucleation and/or crystallization effect in the amorphous fraction of the polymer prevented the molecular dispersion of the drug in the matrix.

CONCLUSIONS

$SCCO_2$ was used in this work for the solvent-induced crystallization of L-PLA of low and high molecular weight as well as for their thermal annealing and crystallization from the melt. The use of $SCCO_2$ dropped the T_g, T_c, and T_m of the raw material during processing. Treatment with $SCCO_2$ at different temperatures allowed obtaining L-PLA samples having different structures with respect to the crystallinity, crystallite size, and crystal morphology. Three different behaviors were observed: (i) at temperatures near the glass transition temperature of the raw polymer a solvent-induced crystallization process was provoked by the presence of $SCCO_2$; (ii) at temperatures between the glass transition temperature and the cold crystallization temperature of the raw polymer, isothermal annealing leading to a seeded nucleation process of the polymer chains in the amorphous region was more likely to occur; and (iii) at temperatures between the cold crystallization and the melt of the raw polymer, nucleation and crystallization from the melt was provoked during simultaneous system depressurization and cooling. For the semicrystalline L-PLA, the induced nucleation and/or crystallization effect in the amorphous fraction prevented the molecular dispersion of organic compounds (such as triflusal) in the matrix.

References

1. Södegård, A.; Stolt, M. Prog Polym Sci 2002, 27, 1123.
2. Proikakis, C. S.; Tarantili, P. A.; Andreopoulos, A. G. J Elast Plast 2002, 34, 49.
3. Drumright, R. E.; Gruber, P. R.; Henton, D. E. Adv Mater 2000, 12, 1841.
4. Lunt, J. Polym Degrad Stab 1998, 59, 145.
5. Weir, N. A.; Buchanan, F. J.; Orr, J. F.; Farrar, D. F.; Boyd, A. Biomaterials 2004, 25, 3939.
6. Freitas, M. N.; Marchetti, J. M. Int J Pharm 2005, 295, 201.
7. Tsuji, H.; Ikada, Y. Polymer 1995, 36, 2709.
8. Ohtani, Y.; Okumura, K.; Kawaguchi, A. J. Macromol Sci B 2003, 42, 875.
9. Puiggali, J.; Ikada, Y.; Tsuji, H.; Cartier, L.; Okihara, T.; Lotz, B. Polymer 2000, 41, 8921.
10. Zhang, J.; Tsuji, H.; Noda, I.; Ozaki, Y. Macromolecules 2004, 37, 6433.
11. Tsuji, H.; Takai, H.; Saha, S. K. Polymer 2006, 47, 3826.
12. Kulinski, Z.; Piorkowska, E. Polymer 2005, 46, 10290.
13. Fleming, S.; Kazarian, S. G. In Supercritical Carbon Dioxide in Polymer Reaction Engineering; Kemmere, M. F, Meyer, T, Eds.; Wiley-VCH: Weinheim, 2005; p 205.
14. Bahrami, M.; Ranjbarian, S. J Supercrit Fluids 2007, 40, 263.
15. Ganapathy, H. S.; Hwang, H. S.; Jeong, Y. T.; Lee, W. K.; Lim, K. T. Eur Polym J 2007, 43, 119.
16. Bratton, D.; Brown, M.; Howdle, S. M. Macromolecules 2003, 36, 5908.
17. Khan, F.; Czechura, K.; Sundararajan, P. R. Eur Polym J 2006, 42, 2899.
18. Jenkins, M. J.; Harrison, K. L.; Silva, M. M. C. G.; Whitaker, M. J.; Shakesheff, K. M.; Howdle, S. M. Eur Polym J 2006, 42, 3145.
19. Shieh, Y. T.; Su, J. H.; Manivannan, G.; Lee, P. H. C.; Sawan, S. P.; Spall, W. D. J Appl Polym Sci 1996, 59, 695.
20. Shieh, Y. T.; Su, J. H.; Manivannan, G.; Lee, P. H. C.; Sawan, S. P.; Spall, W. D. J Appl Polym Sci 1996, 59, 707.
21. Takada, M.; Tanigaki, M.; Ohshima, M. Polym Eng Sci 2001, 41 1938.
22. Gupper, A.; Chan, K. L. A.; Kazarian, S. G. Macromolecules 2004, 37, 6498.
23. Takada, M.; Hasegawa, S.; Ohshima, M. Polym Eng Sci 2004, 44, 186.
24. Stejny, J.; Whitfield, A. F.; Pritchard, G. M.; Hill, M. J. Polymer 1998, 39, 4175.
25. Lillie, E.; Schulz, R. C. Die Makromol Chem 1975, 176, 1901.
26. Espartero, J. L.; Rashkov, I.; Li, S. M.; Manolova, N.; Vert, M. Macromolecules 1996, 29, 3535.
27. de Jong, S. J.; Arias, E. R.; Rijkers, D. T. S.; van Nostrum, C. F.; Kettenes-van den Bosch, J. J.; Hennink, W. E. Polymer 2001, 42, 2795.
28. González, M. F.; Ruseckaite R. A.; Cuadrado, T. R. J Appl Polym Sci 1999, 71, 1223.
29. Agarwal, M.; Koelling, K. W.; Chalmers, J. J Biotechnol 1998, 14, 517.
30. Kopinke, F. D.; Remmler, M.; Mackenzie, K.; Möder, M.; Wachsen, O. Polym Degrad Stab 1996, 53, 329.
31. Jameel, H.; Waldman, J.; Rebenfeld, L. J Appl Polym Sci 1981, 26, 1795.
32. Chiou, J. S.; Barlow, J. W.; Paul, D. R. J Appl Polym Sci 1985, 30, 3911.
33. Fischer, E. W.; Sterzel, H. J.; Wegner, G. Kolloid Z Z Polym 1980 1973, 251.
34. Li, S. M.; Garreau, H.; Vert, M. J Mater Sci Mater Med 1990, 1, 198.
35. Kriese, M. D.; Boismier, D. A.; Moody, N. R.; Gerberich, W. W. Eng Fract Mech 1998, 61, 1.
36. Todo, M.; Shinohara, N.; Arakawa, K. J Mater Sci Lett 2002, 21, 1203.
37. Park, S. D.; Todo, M.; Arakawa, K.; Koganemaru, M. Polymer 2006, 47, 1357.
38. von Schnitzler, J.; Eggers, R. J Supercrit Fluids 1999, 16, 81.
39. Mohamed, A. A.; Gordon, S. H.; Carriere, C. J.; Kim, S. J Food Qual 2006, 29, 266.
40. Van Landingham, M. R.; Villarrubia, J. S.; Guthrie, W. F.; Meyers, G. F. Macromol Symp 2001, 167, 15.
41. Elvira, C.; Fanovich, A.; Fernandez, M.; Fraile, J.; San Roman, J.; Domingo, C. J Controlled Release 2004, 99, 231.